Journal of the Korean Institute of Illuminating and Electrical Installation Engineers (2014) 28(5) : 106~114
http://dx.doi.org/10.5207/JIEIE.2014.28.5.106 ISSN 1229-4691(Print) ISSN 2287-5034(Online)

논문 28-5-13

Design to Reduce Cost and Improve the Mechanical Durability of IPMSM in Traction Motors

Ki-Doek Lee* · Ju Lee**

Abstract

The interior permanent-magnet synchronous motor (IPMSM) is often used for the traction motor of hybrid electric vehicles (HEVs) and electric vehicles (EVs) due to its high power density and wide speed range. This paper introduces the 120kW class IPMSM for traction motors in military trucks. This system, as a SHEV (series hybrid electric vehicle), requires a traction motor that can generate high torque. This study introduces a way to reduce costs by proposing a design approach that creates reluctance torque that can be maximized by varying the dq-axis inductance. If a model designed by a design approach meets the desired torque, the magnetic torque can be reduced by an amount equal to the increase in reluctance torque and consequently the amount of permanent magnets can be reduced. A reduction gear and high speed operation of motors are necessary for the miniaturization of the motor. Thus, a fairly large centrifugal force is generated due to the high speed rotation. This force causes mechanical interference between the rotor and the stator, and a design approach for adding an iron bridge is explained to solve the interference. In this study, the initial model and the improved model that reduces cost and improves mechanical durability are compared by FEA, and the models are produced. Finally, the FEM results were verified experimentally.

Key Words : PMSM, IPMSM, Traction Motor

1. Introduction

The main application of an interior permanent magnet synchronous motor (IPMSM) is a traction motor for fuel cell electric vehicles, hybrid electric vehicles, and battery electric vehicles. The hybrid vehicle systems are divided into three parts: SHEV (series hybrid electric vehicle), PHEV (parallel hybrid electric vehicle) and PSHEV (power split hybrid electric vehicle). Among them, the SHEV should operate all driving areas of the vehicle by pure motor propulsion. For this reason, SHEV requires a higher torque than other systems[1]. This paper introduces a 120kW class IPMSM for a traction motor of series hybrid military trucks.

* Main author : Department of Electrical Engineering, Hanyang University
** Corresponding author : Department of Electrical Engineering, Hanyang University
Tel : +82-2-2220-0349, Fax : +82-2-2295-7111
E-mail : leekidoek@naver.com
Date of submit : 2014. 3. 15
First assessment : 2014. 3. 19
Completion of assessment : 2014. 4. 14

Because the costs of neodymium and dysprosium, which are main materials in the NdFeB magnet, have been increasing, a competitive price for the PMSM is indeed a consideration. As a result, a design approach that fulfills the needed torque and reduces the amount of permanent magnet is needed. Because of rotor saliency, an IPMSM generates additional reluctance torque as well as magnetic torque [2-3]. The torque per amount of PM (permanent magnet) can be maximized by the maximizing reluctance torque, which changes according to the dq-axis inductance. Because the dq-axis inductance is a changing value according to the rotor shape, a design that increases the torque per the amount of PM is accomplished by a dq-axis inductance analysis according to rotor shape.

The traction motor for HEVs is equipped with an internal combustion engine unlike the traction motor for EVs. Because of the limited space of HEVs, a minimal motor size is important. To meet the size constraints on the motor, a PMSM should be utilized, as high speed and a reduction gear is needed. However, the high speed operation will cause a fairly large centrifugal force on the rotor, and this force may cause mechanical problems [4-6]. In this study, these problems are addressed and a design approach explained that will help resolve the issue.

2. Requirements and Constraints

In this paper, the traction motor of a SHEV system for 5 ton class military trucks is introduced. The rolling, air drag and slope resistance considering the harsh operating conditions within which military trucks are utilized were calculated. The reduction gear and instantaneous rating were considered to reduce the motor size, and the final load points considering these were determined. Table 1 represents the required load characteristics at rated speed and maximum speed. Table 2 represents the required constraints in the design of a traction motor.

Table 1. Desired Torque and Speed

Specifications		Value	Unit
Instantaneous rating (1 min)	Power	120	kW
	Desired torque @ rated speed	403 @ 2,843	Nm @ rpm
	Desired torque @ maximum speed	115 @ 10,000	Nm @ rpm
Continuous rating (60 min)	Power	65	kW
	Desired torque @ rated speed	218 @ 2,843	Nm @ rpm
	Desired torque @ maximum speed	62 @ 10,000	Nm @ rpm

Table 2. Required Constraints

Specifications	Value	Unit
Maximum phase current	500	Apeak
Slot fill factor (pure copper)	35	%
Phase voltage limit	346	Vpeak
Core	S08	-
Permanent magnet	38UH	-
Current density	15	Apeak/mm2
Temperature	180	degree
Pole/slot	8/12	-
Cooling	Water cooling	-

3. Machine Design And Problem

A motor size that satisfies the desired torque-speed and constraints can be designed by the magnetic equivalent circuit and output equation. Fig. 1 shows the flow chart for PMSM design.

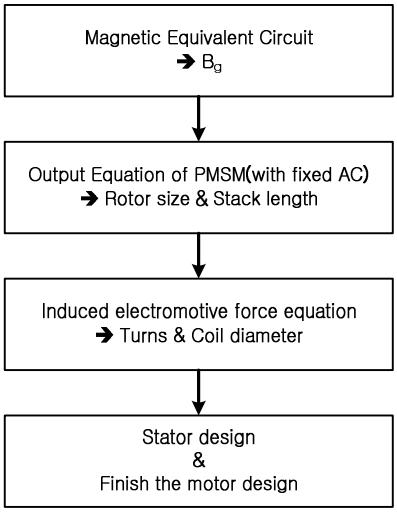

Fig. 1. Flow chart for PMSM design

In the first step, the air gap flux density is calculated from the magnetic equivalent circuit of the PMSM. The air gap flux density, which does not consider the leakage flux of the rib, can be represented as Formula (1) through the simplified magnetic equivalent circuit [2].

$$B_g = \frac{k_{lb}k_{ls}}{1+k_r\frac{g'\mu_R}{T_m}}B_r \tag{1}$$

Where k_{lb} is the barrier leakage coefficient, k_{ls} is the air gap leakage coefficient, k_r is the reluctance coefficient, g` is the air gap length considering carter's coefficient, μ_R is the relative permeability of permanent magnet, T_m is the magnet thickness, B_r is the residual magnetic flux density of permanent magnet.

The variables k_{lb}, k_{ls}, k_r, g`, μ_R, T_m, B_r can be determined by the initial setting and experience.

In the second step, the rotor size is calculated. If the desired torque is calculated by load condition and the specific electric loading ac is fixed, the rotor size can be calculated by Formula (2). ac is the $I_aZ/\pi D_g$ and is called the specific electric loading.

$$T_m = \left(\frac{\pi}{4}k_w\hat{B}_{g1}ac\cos\beta\right)D_g^2L_{stk} \tag{2}$$

Where k_W is the winding factor, $\hat{B}_{g1}$ is the peak value of the fundamental wave of air gap flux density, β is the current phase angle, D_g is the diameter of air gap, L_{stk} is the stack length.

The variable $k_w, \hat{B}_{g1}, \beta$ of the expression (2) can be determined by the previous calculation and required constraints.

In the third step, the coil diameter and the number of stator coils are calculated. If the induced voltage at zero load is established by the required constraints, the number of stator coils can be calculated by the expression (3).

$$N_{ph} = \frac{E_0}{k_w\omega_r\phi_{g1}} \tag{3}$$

Where N_{ph} is the number of series turns per phase, E_0 is the zero load EMF (electromotive force), ϕ_{g1} is the air gap flux per poles, ω_r is the rated angular velocity.

If the number of stator coil is calculated by Formula (3), the magnitude of current can be determined through ac. If the magnitude of current is calculated, the coil diameter can be calculated by the current density in constraints.

In the fourth step, the stator design is performed by the previously obtained value and the basic design of the motor can be completed.

The characteristic analysis of the initial model and the shape design were performed, and the experiment was also performed after production. The design approach, which reduces the price of PMSM, was performed in the shape design by FEA. As a result of these experiments, the torque-speed requirements were met, but mechanical difficulties

were encountered. The centrifugal force of the rotor generated by the high speed operation, which allows for the miniaturization of the motor, and an insufficient fixation of the rotor with permanent magnets cause mechanical interference. Fig. 2 (a) represents the FEA model, and Fig. 2 (b) represents the rotor that caused mechanical interference with the stator. A design approach for resolving this mechanical problem will be explained in the next section.

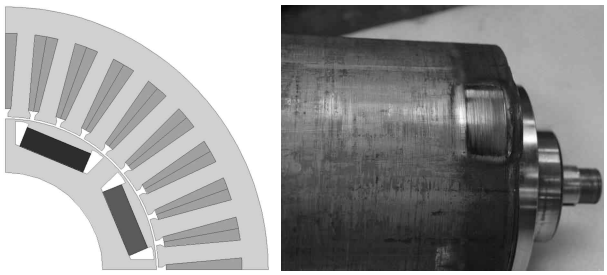

Fig. 2. (a) FEA model (b) Rotor with mechanical interference

4. Design Approaches by FEA

4.1 Design Approach 1

In order to reduce the cost of the model that was designed in the flow chart, the amount of permanent magnets had been reduced through Design Approach 1. The magnetic torque is reduced depending on the amount of permanent magnet. If the reluctance torque that is generated by rotor saliency increases, the reduced torque can be complemented. Fig. 3 represents the initial model and design variables, and Fig. 4 represents the dq-axis flux path of IPMSM.

The d-axis inductance of IPMSM is determined by the thickness of the magnet, and q-axis inductance is determined by web width. The reluctance torque is generated by the magnitude of L_q-L_d. The L_d can be reduced by the increase of magnet thickness, but this method is inadequate as it comes with a high cost. Because the increased web width that causes the decrease of q-axis reluctance and thus increases the L_q, this approach can consequently reduce the price and increase the reluctance torque. Torque and dq-axis inductance of the four models which differ from magnet width and web width were analyzed by FEA.

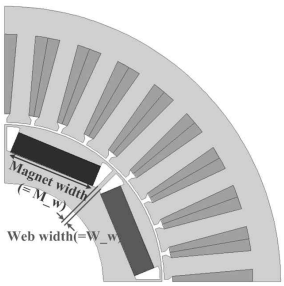

Fig. 3. Initial model and design variables

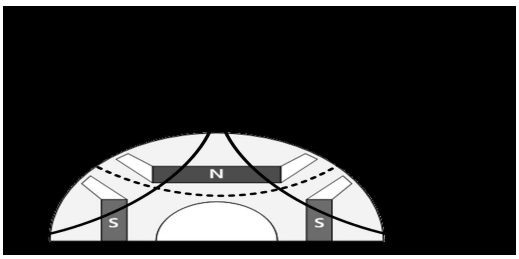

Fig. 4. dq-axis flux path

Table 3. Design Variables and Output Characteristics of the Four Models

	Model 1	Model 2	Model 3	Model 4
Magnet Width[mm]	41.8	37.5	34	30.5
Web Width[mm]	2	6.5	10	13.7
L_d[mH]	0.255	0.251	0.251	0.256
L_q[mH]	0.410	0.469	0.499	0.515
L_q/L_d	1.61	1.87	1.98	2.01
Torque[Nm]	434.54	439.29	434.64	418.12

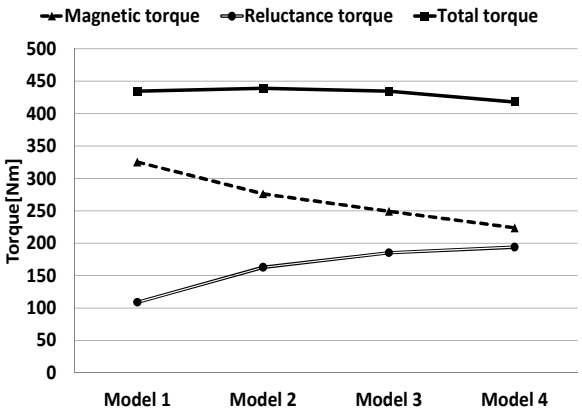

Fig. 5. Torque analysis of four models

Table 3 represents the torque and dq-axis inductance of the four models. Because the magnet thickness, which is the d-axis flux path, does not change, the L_d value of the four models are very similar. In Table 3, the rotor saliency of the four models is different because the L_q is changed by web width. Although the magnetic torque is decreased by reducing the width of the permanent magnet, the total torque of models 1, 2, and 3 are almost the same. For this reason, the reluctance torque has been increased by the same amount that the magnetic torque has been reduced. As shown in Table 3, the amount of permanent magnet in Model 3 decreased about 81% than Model 1, but torque remains constant. The cost decreases by a design approach in which the amount of permanent magnet used is reduced. The reluctance torque, magnetic torque and total torque of each model are shown in Fig. 5. The rotor saliency of Model 4 does not increase further. For this reason, the reluctance torque of Model 4 is not increased and thus the decrease of its total torque has been verified.

4.2 Design Approach 2

If the rotor operates at high speed, a large centrifugal force is induced. The tensile stress in the rotor core is generated by the centrifugal force. If the tensile stress is greater than the yield stress, permanent deformation (plastic deformation) occurs. When performing the experiment on the initial model, permanent deformation occurred because the permanent magnet and rotor core had not been properly fixed[4-6]. In addition, elastic deformation could occur even without causing permanent deformation. For this reason, a model that has the robust structure of mechanical deformation has been redesigned by the electromagnetic analysis and mechanical stress analysis. When a stress analysis is performed, the mechanical coefficients are found as follows:

- Rotor: Young's modulus 162.4GPa, Poisson's ratio 0.33, Yield point 440MPa
- Magnet: Young's modulus 140GPa, Poisson's ratio 0.24, Tensile strength 120Mpa

In addition, the no load rotation condition is 12,000rpm. The boundary condition of the permanent magnet and the rotor considering construction is shown in Fib. 6 below. Table 4 represents the design variables for FEA and the desired characteristics of the IPMSM. The safety factor was calculated as (Yield point/Stress).

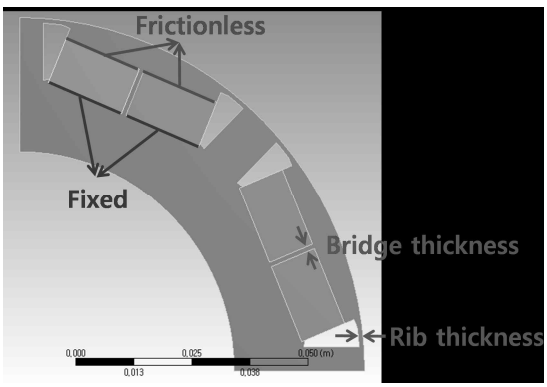

Fig. 6. Design variables and boundary condition

Table 4. Design Variables for FEA and Desired Characteristics

	Item	Specification	Unit
Design Variables	Bridge	0~2(step:0.5)	mm
	Rib	1~2(step:0.2)	mm
	Air gap	1~1.5(step:0.1)	mm
Condition	Speed	12,000	RPM
Desired value	Torque	403↑	Nm
	Safety factor	2↑	

First, the width of the permanent magnet was separated into two pieces with an iron bridge added between the two pieces. The results, which represent the electromagnetic analysis and the mechanical stress analysis of Bridge 0, 0.5, 1, 1.5, 2 mm models, are shown in Fig. 7. The leakage flux on the bridge is increased by increasing the bridge thickness, so the torque tends to decrease. The safety factor was less than 1 at a 1mm bridge model, but the safety factor of a 0.5mm bridge model increased to approximately 2. The safety factor from a 0mm to a 1mm bridge increased significantly. However, the safety factor of the 1.5 and 2 mm models was almost equal to the 1 mm bridge model. Because the 1mm bridge model satisfies the desired torque, this bridge was applied to the initial model. Fig. 8 represents the results of the stress analysis of the no-bridge model and 1 mm bridge model.

The maximum stress point of the no-bridge model was the rib areas. The FEA results (Fig. 9) were analyzed depending on increasing rib thickness in order to counter the force. The leakage flux increased due to the increased thickness of the rib, and thus torque was significantly reduced. Unlike bridge thickness, rib thickness did not have a significant effect on safety factors. For this reason, the 1mm rib was determined as existing.

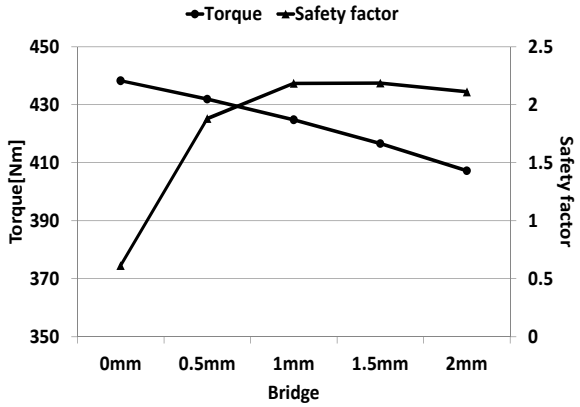

Fig. 7. Torque and safety factor according to the bridge thickness

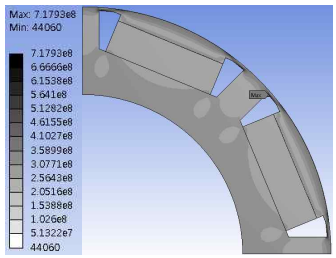

(a)

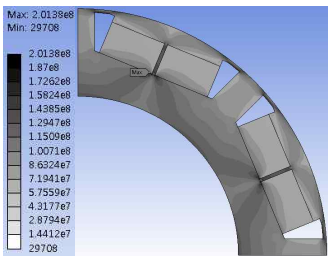

(b)

Fig. 8. Stress analysis results
(a) No-bridge (b) 1mm bridge

The expansion and reduction at the rotor are repeated by elastic deformation even if plastic deformation does not occur. To prevent interference between the stator and rotor due to deformation, the output characteristics (Table 5) were analyzed depending on increasing the air gap length. The operating point of the permanent magnet was lowered when air gap length was increased, and

torque was consequently reduced. The 1.2mm air gap model considering the torque margin as a tolerance and a stray-load loss was determined as the improved model.

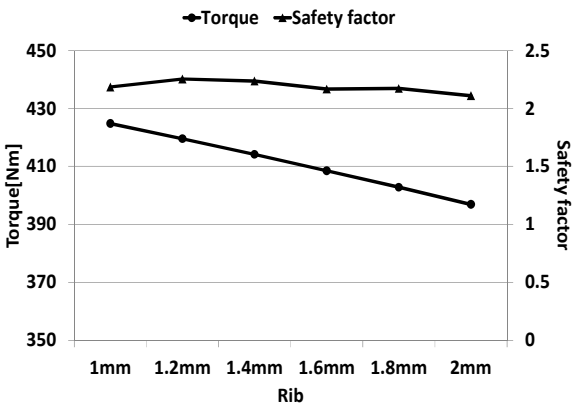

Fig. 9. Torque and safety factor according to rib thickness

Table 5. Torque according to the Air Gap Length

	1mm	1.1mm	1.2mm	1.3mm	1.4mm	1.5mm
Torque	424.79	418.15	411.57	404.41	397.43	390.75

5. Comparison of Initial Model and Improved Model

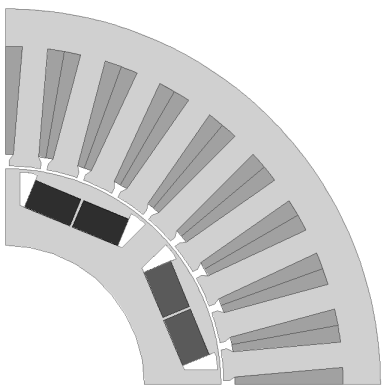

Fig. 10. Improved model for FEA

Fig. 10 represents the improved model. Table 6 represents the comparison data of the initial model and the improved model. As a result, the amount of the permanent magnet was reduced and thus the motor price is reduced. The improved model, which has a 1.2mm air gap and additional 1mm bridge, shows improved mechanical durability and meets the desired torque.

Table 6. Comparison of Initial Model and Improved Model

Specification		Initial Model	Improved Model	Unit
Design	Magnet width	41.8	34	mm
	Web width	2	10	mm
	Bridge	0	1	mm
	Air gap	1	1.2	mm
Characteristics	Torque	434.54	411.57	Nm
	Torque / Magnet width	10.4	12.105	Nm/mm
	Safety factor	0.61	2.18	

6. Experimental Results

Figs. 11 and 12 represent the prototype of the improved model and the test set. Fig. 13 and Table 7 represent the zero-load back-emf at 3,000 rpm compared to the FEA data and experiment data. In addition, mechanical durability was verified through an aging test.

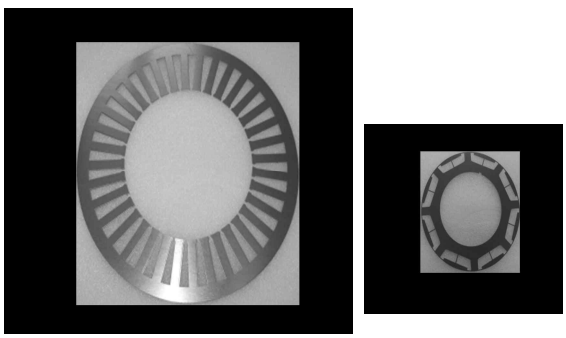

Fig. 11. Stator and rotor of improved model

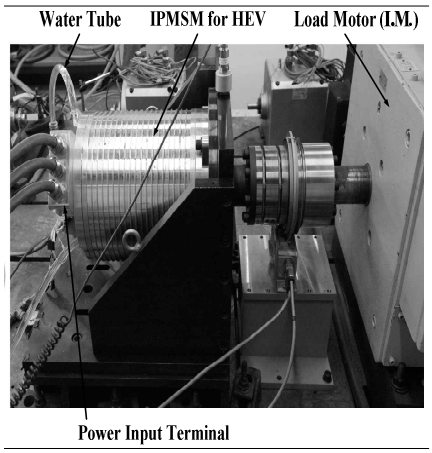

Fig. 12. Test set

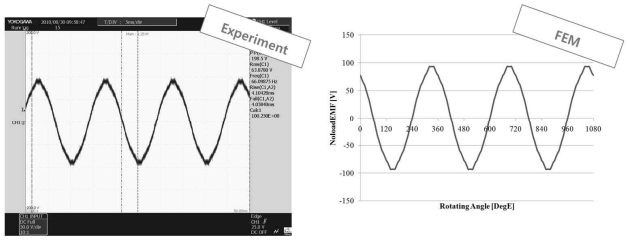

(a) (b)

Fig. 13. Zero-load back-emf at 3,000 rpm
(a) Experiment (b) FEM

Table 7. Comparison of FEM and Experiment

	RMS	Fundamental Harmonics	5th/1th	7th/1th	THD
Experiment	63.88V	87.76V	2.36%	0.95%	2.87%
FEM	64.51V	91.25V	2.50%	0.83%	2.82%
Error	0.98%	3.82%	0.14%	0.12%	0.05%

7. Conclusion

This study introduced a 120kW class IPMSM for the traction motors of SHEV military trucks. In the basic design, a model having excellent electromagnetic performance except for mechanical durability was designed. To reduce cost, a design approach that can increase the reluctance torque was undertaken. This design approach could reduce the amount of permanent magnet needed. The produced motor sustained damaged due to the high centrifugal force during the high speed rotation experiment. To compensate for this, the improved model, which provides the desired torque and improves mechanical durability, was designed by an FEA of electromagnetic analysis and stress analysis. The FEA analysis results of the improved model were adequately verified through experiment.

ACKNOWLEDGMENT

This work was supported by the National Research Foundation of Korea grant funded by the Korean government under Grant 2013R1A2A1A01015171.

References

[1] Sung Chul Oh, "Evaluation of Motor Characteristics for Hybrid Electric Vehicles Using the Hardware-in-the-Loop Concept," IEEE Trans. Veh. Technol., Vol. 54, Issue 3, pp. 817-824, May. 2005.
[2] Hyung-Woo Lee, Ki-Doek Lee, Won-Ho Kim, Ik-Sang Jang, Mi-Jung Kim, Jae-Jun Lee and Ju Lee, "Parameter Design of IPMSM With Concentrated Winding Considering Partial Magnetic Saturation," IEEE Trans. Magn., Vol. 47, Issue 10, pp. 3653-3656, Oct. 2011.
[3] THOMAS M. JAHNS, GERALD B. KLIMAN and THOMAS W. NEUMANN, "Interior Permanent-Magnet Synchronous Motors for Adjustable-Speed Drives," IEEE Trans. Ind. Appl., Vol. IA-22, Issue 4, pp. 738-747, Jul./Aug. 1986.
[4] Jae-Woo Jung, Byeong-Hwa Lee, Do-Jin Kim, Jung-Pyo Hong, Jae-Young Kim, Seong-Min Jeon, Do-Hoon Song, "Mechanical Stress Reduction of Rotor Core of Interior Permanent Magnet Synchronous Motor," IEEE Trans. Magn., Vol. 48, Issue 2, pp.911-914, Feb. 2012.
[5] Dutta, R, Rahman, M.F, "Design and Analysis of an Interior Permanent Magnet (IPM) Machine With Very Wide Constant Power Operation Range," IEEE Trans. Energy Conversion, Vol. 23, Issue 1, pp. 25-33, Mar. 2008.
[6] Katsumi Yamazaki and Yusuke Kato, "Optimization of High-Speed Motors Considering Centrifugal Force and Core Loss Using Combination of Stress and Electromagnetic Field Analyses," IEEE Trans. Magn., Vol. 49, Issue 5, pp.2181-2184, May. 2013.

Biography

Ki-Doek Lee

Mr. Lee received a B.S. degree in electrical engineering from Incheon University. He received an M.S. degree in electrical engineering from Hanyang University. Since 2011, he has been pursuing a Ph.D. degree in the Department of Electrical Engineering, Hanyang University. His research interests are design, analysis and control of motor/generators; power conversion systems.

Ju Lee

Dr. Lee obtained his B.S. and M.S. degrees from Hanyang University, Seoul, Korea in 1986 and 1988, respectively. He obtained his Ph.D. from Kyusyu University, Fukuoka, Japan, in 1997. He worked as an Assistant Researcher at the Agency for Defense Development from 1989 to 1993 and with the Korea Railroad Research Institute in 1997 as Chief of the Division on Light Subway Systems. He joined Hanyang University as a Professor of the Department of Electrical Engineering in September 1997. His main research interests include electrical machinery and drives; electromagnetic field analysis; new transformation systems, such as hybrid electric vehicles and high-speed electric trains; and standardization. Dr. Lee was recognized by the Japan Electric Society as the writer of the Best Paper in 1995. He is a member of the IEEE Industry Applications Society, Magnetics Society, and Power Electronics Society. He has been a member of the editorial staff of the Korean Institute of Electrical Engineers since 1998 and a member of the editorial board of the International Journal of Electrical Engineering since 2000. In addition, he has been the Korea National Committee Secretary of the IEC/TC2 since 1999. He is also the General Manager of the Human Resource Development Center for Electric Machine and Devices, Seoul, Korea.